Soft Matter

COMMUNICATION

View Article Online
View Journal

Cite this: DOI: 10.1039/c5sm01136a

Received 11th May 2015,
Accepted 3rd August 2015

DOI: 10.1039/c5sm01136a

www.rsc.org/softmatter

Dielectric discontinuity in equilibrium block copolymer micelles

Alexander V. Korobko,[a] Carlos M. Marques,[b] Matthias Schöps,[c] Volker Schädler,[d] Ulrich Wiesner[e] and Eduardo Mendes*[ae]

The surface tension between the hydrophobic core and the solvent is known to play a major role in the self-assembly of diblock copolymer micelles in solution. Coulombic forces are also very important in the case of aggregates with weakly charged coronas. The aggregation number and morphology are often tuned by the addition of electrolytes to the solution *via* electrostatic screening and an eventual change in solvent quality. However, when the surface tension is low enough, dielectric discontinuity between the core and the solvent becomes important enough in comparison to other mechanisms, driving the surface tension at the same time it screens electrostatic interactions in the corona. Below, we demonstrate the importance of this effect for micelles with neutral and weakly charged coronas.

In selective solvents, amphiphilic neutral and polyelectrolyte diblock copolymers spontaneously form micellar structures consisting of a solvophobic core surrounded by the solvent soluble corona.[1–3] Neutral micelles in equilibrium presume the core to be liquid, and the high mobility of the core forming blocks ensures the core size to be driven by elastic forces of solvophobic blocks and the surface tension between the liquid core and the solvent. Corona chains contribute *via* osmotic pressure (stretching the corona blocks) as well as *via* electrostatics in the case charged moieties are present on the corona chains.[4–7] By altering the solvent quality or/and screening the Coulomb repulsion between charges, the micellar core adjusts and the micelle is prone to morphological changes.[8–11]

Electrostatic interactions are usually tuned by the addition of salts. For charged polyelectrolyte chains of the corona, an increase of ionic strength in the solvent provides chain conformational changes that may go from the rod-like shape to the fully collapsed globule[12] in the most extreme cases. In reality, a change in the ionic strength of the solution also affects the surface tension between the core and the solvent. As the dielectric constant is different between the core and the solvent establishing a dielectric discontinuity, the presence of added salt ions at the solvent–core interface builds up a charge profile. That interfacial charge density change implies a change in interfacial energy which in turn reflects in a surface tension. The magnitude of this effect is proportional to the jump of dielectric constant, $\varepsilon_s - \varepsilon_c$, across the Gibbs dividing surface. The excess of surface tension between the liquid core and the solvent is given by the Gibbs adsorption isotherm equation, $d\gamma = -\sum_{i=1}^{n} \Gamma_i d\mu_i$ written for n species of ions with chemical potential μ_i. The integrated ion number density profile derives the ion excess/depletion at the interface in relation to the bulk, Γ_i, and establishes the decrease/increase of the surface tension.

The small surface tension between the micelle core and the solvent is accompanied with a weakening of the segregation due to penetration of the solvent into the core. The classic example is the self-consistent mean-field theory prediction, where for the weakly segregated domains the width of the core interface is large, the interfacial tension is low, and polymers resemble unperturbed Gaussian chains.[13–15]

Most of studies in the literature, however, consider situations where the surface tension between the core and the solvent is very high as very hydrophobic blocks are used in the core. The motivation for the present study is to consider an experimental situation where we can probe the competition between these two effects: we consider a system with very few ionic moieties attached to the corona (only one or two groups per chain) implying in a very low charge density around the core, but at the same time, we consider a core–solvent combination in which the surface tension is very low, implying that an ion-induced increment to the surface tension can also be large. The amplitude of the latter effect is obtained by also studying the aggregation of non-charged micelles that possess the same molecular weight.

[a] Department of Chemical Engineering, Delft University of Technology, Julianalaan 136, 2628 BL Delft, The Netherlands. E-mail: E.Mendes@tudelft.nl
[b] Institut Charles Sadron, Université de Strasbourg, CNRS UPR22, F-67034 Strasbourg, France
[c] BASF Coatings AG, P.O. Box 6123, 48136 Muenster, Germany
[d] BASF Polyurethanes GmbH, Elastogranstraße 60, 49448 Lemförde, Germany
[e] Materials Science & Engineering, Cornell University, 329 Bard Hall, Ithaca, NY, 14853-1501, USA

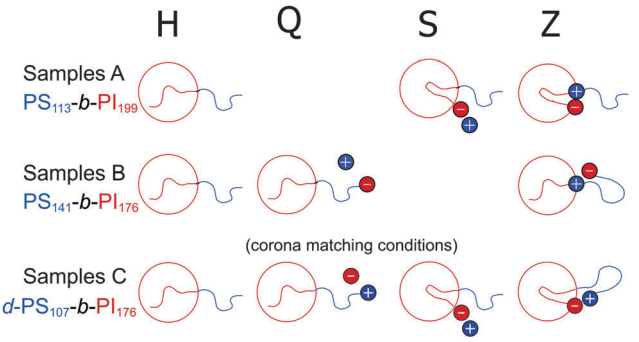

Fig. 1 Micellar assemblages from macrosurfactants of different architectures and block lengths used in this study (no added salt): neutral block-copolymer (H); end-capped PS block (Q); end-capped PI block (S); and zwitterionic architecture (Z). The polymerization degree of every polymer family is denoted by letters A, B and C, while the charge sign and positioning by letters H, Q, S and Z. Every sample in thus study is named after a combination of these two sets of letters. Samples A and B are fully hydrogenated while the polystyrene (PS) block of sample C is fully deuterated.

In order to achieve this we report below a neutron scattering study on partially deuterated or non-deuterated, neutral and ionically end-capped poly(styrene-*b*-isoprene) [PS_n-*b*-PI_m] diblock copolymers in a barely poor solvent for PI, dimethylacetamide (DMAc). Here, n and m denote degrees of polymerization of the PS and PI blocks, respectively. The n and m values used in this work are explicitly given in Fig. 1. DMAc is polar enough to still allow corona electrostatics to play an important role.

Partially deuterated poly(styrene-*b*-isoprene) (d-PS-*b*-PI) block copolymers with end-capped ionic group(s) were synthesized by sequential anionic polymerization.[16] The selectivity of polar solvent (dimethylacetamide, Cambridge Isotopes Laboratories) to the PI block and functionalized end-groups (the quaternized amine group at the end of PS chain or/and the sulfonated end group of the PI block) drives macrosurfactants to form spherical micelles with a PI liquid core and a PS corona, Fig. 1. Here micelles formed from the neutral (non-modified) diblock copolymers (H) were chosen as a reference. Q refers to micelles with a charged PS-end group (the positively charged quaternized amine group or the negatively charged sulfonate group). S corresponds to micelles with a charged core surface (irrespectively of the charge sign); Z denotes micelles assembled from charge–charge associative zwitterions, in contrast to the permanent PS-*b*-PI block copolymers.[17,18] To measure the core size directly, the neutron scattering signal from corona d-PS blocks was matched with the solvent by mixing deuterated and hydrogenated DMAc in an appropriate ratio (sample C). Samples A and B were prepared in deuterated DMAc without contrast matching, and therefore allowing for the scattering from the corona. The neutron scattering length density of PS for a density of $\rho = 1.034$ g cm^{-3} was calculated to be $\rho_{PS} = 1.389 \times 10^{10}$ cm^{-2}, whereas $\rho_{d\text{-}PS} = 6.412 \times 10^{10}$ cm^{-2} is for fully deuterated PS with a density of 1.12 g cm^{-3}. Polyisoprene with $\rho = 0.97$ g cm^{-3} and $\rho_{PI} = 0.283 \times 10^{10}$ cm^{-2} was in use.[19,20] The neutron scattering length density of DMAc with $\rho = 0.937$ g cm^{-3} was $\rho_{DMAc} = 4.883 \times 10^{10}$ cm^{-2}, and for the deuterated DMAc of density 1.03 g cm^{-3} calculations give $\rho_{d\text{-}DMAc} = 7.877 \times 10^{10}$ cm^{-2}.

A solution of LiCl salt in the appropriate DMAc was added to the initial micellar solution in proportions to achieve the salt concentration in the range of 0.003–0.1 M and the fixed concentration of a polymer, 1 wt%. The static dielectric constant of the PI core is $\varepsilon_{PI} = 3$, whereas $\varepsilon_{DMAc} = 37.8$. LiCl is soluble in polar solvent DMAc and commonly used in organic synthesis. In the synthesis procedure for the polymers used in our paper, the ionically end-functionalized group of polyisoprene is a lithium sulfonated group, where Li^+ is a counter ion of the SO_3^- group. Therefore, we have chosen to use LiCl as a salt.

Small angle neutron scattering profiles of micellar solution were measured using the PAXY diffractometer at LLB (CEA Saclay) and using spectrometer D11 at ILL (Grenoble), France. An incident wavelength of $\lambda = 10$ Å and $\lambda = 7$ Å and a range of the effective sample-detector distance were chosen to ensure a momentum transfer range of 0.006–0.1 Å^{-1}.

To model the form factor of micelle, $P_m(q;R_c,R_g)$, the core of micelles is described as a homogeneous dense sphere of PI blocks with radius R_c and the corona is represented by Gaussian chains with the radius of gyration R_g attached to the core.[21] We assume that the thickness of the corona layer, $R_s = 2R_g$. Despite the soft nature of the micellar corona, the inter-micelle interaction was approximated with a hard-sphere potential. The Percus–Yevick approach for the closure relation was employed to derive the solution structure factor, $S(q;R_{hs})$, of "effective" hard spheres of radius R_{hs} and a volume fraction φ.[22,23] Thus, R_{hs} reflects the dimension of the micelle and the magnitude of electrostatic interaction between micelles.

To recover effective values of R_{hs}, φ as well as R_c and R_g, the experimental scattering profiles were fitted to the modeled SANS spectra

$$I_m(q) \sim \int_0^\infty P_m(q; R_c, R_g) S(q; R_{hs}) f(R_c; \overline{R}_c, \sigma) \mathrm{d}R_c, \qquad (1)$$

with the local monodisperse approximation and the Levenberg–Marquardt non-linear least-squares fitting algorithm.[21] The polydispersity of the core was evaluated by the Gaussian distribution function, $f(R_c;\bar{R}_c,\sigma)$, with the average size $\bar{R}_c$ and dispersion σ.

The experimental SANS profiles and the model fit are displayed in Fig. 2a for the micellar solution of d-PS_{107}-*b*-PI_{176} with no salt (top panel) and 0.1 M (bottom panel) of LiCl. In the absence of a salt, the inter-micellar correlation peaks appear only for micelles with ionically end-capped PS or PI blocks (Q and S samples). The origin of the peak is purely electrostatic, as at 0.1 M LiCl the peak disappears and the scattering spectra of the Q and S samples match the spectra of micelles with H and Z architectures respectively. Neutral micelles (H samples) reveal no strong intermicellar correlation due to the small polymer concentration. The structure of zwitterionic micelles (Z samples) at 0 M salt concentration resembles the structure of neutral micelles, as the charge–charge complexes of amine and sulfonate groups neutralize the net charge of zwitterions.

The structure factor of the solution $S(q)$ is sensitive to the LiCl salt if macrosurfactant contains charged moieties. The effective hard sphere radius, R_{hs}, of neutral micelles is not affected by the salt, Fig. 3a. However, for micelles with end-capped PS

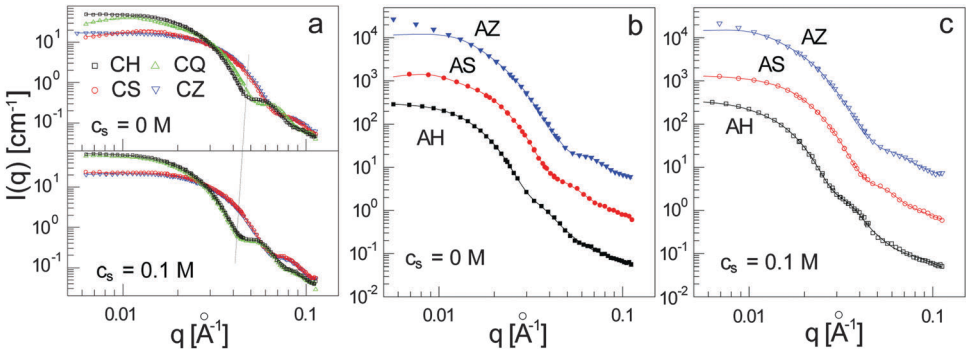

Fig. 2 (a) Scattering intensity profiles for d-PS_{107}-*b*-PI_{176} micellar solution with different macrosurfactant architectures under corona contrast matching conditions for c_s = 0 M (top panel) and c_s = 0.1 M (bottom panel). The dashed line shows the shift of spectra, symbols denote the experimental data, and solid lines denote the modeling. (b) Scattering intensity profiles for PS_{113}-*b*-PI_{199} micelles of different architectures in DMAc without a salt and (c) with 0.1 M LiCl salt. AS and AZ spectra are shifted up for clarity.

blocks (Q samples) or PI block (S sample), single charges at each block are still able to harden the interaction between micelles at low salt concentrations. At about 0.03 M of salt, R_{hs} as well as the structure factor approach the ones of neutral micelles, and the effect of electrostatics disappears. Micelles formed by zwitterions (Z sample) at 0 M salt concentration have the smallest value of R_{hs} among H, Q, S, and Z series, as the charge association between amine and sulphonated end groups condenses PS ends on the PI core making micelles smaller. This association becomes broken by ions of salts, and the released PS end moves away from the core: the micellar size increases and the structure of Z and S micelles becomes very similar.

Fig. 3b shows that the increase of the average core size, $\bar{R}_c$, to the LiCl salt, c_s, is universal despite the variety of the block-copolymer architecture (H, Q, S, Z samples of micelles). Notice, neutral micelles and micelles with charges behave alike, which doubts the charged groups as an explanation of the core size increment. Moreover, the data are split into two groups based on the presence (S, Z) or absence (H, Q) of the charged group at the end of PI block. The high solvent affinity of the sulfonate group fixes the end of the PI chain at the PI–DMAc interface, resulting in micelles with the smaller core size, Fig. 1 (S and Z samples). In the presence of the salt up to 0.1 M, the core size of H and Q micelles is a factor $\simeq 1.4$ larger than the size of the core of S and Z micelles. At 0 M salt concentration, the unscreened charge at the end of the PS chain (Q sample) stretches the chain, and the penalty for this is a reduced core size (from 89 down to 78 Å, green solid line) minimizing the free energy of the micelle. As noted, micelles with the charged core (S micelles) have the same trend of the core size with the salt, which indicates a small effect of charges at the core–solvent interface on the interfacial tension and its increment.

The effect of the PI end-capped sulphonate group on the core size can be estimated assuming that the Gauss stretching energy of the core forming block, F^s_{PI}, is independent of the position of its ends. In other words, there is no change in statistics of the core forming chains if the end of the PI block is moved from any position in the bulk of the core to the core–solvent interface. The end-groups of PI block explicitly fix the chain conformation when both ends are situated on the interface. Keeping the Gaussian stretching energy of the single chain, $F^s_{PI} \sim R_c^2/N_{PI}$, unchanged, we apply the transformation $N_{PI} \mapsto N_{PI}/2$ meaning that by forming the chain loop (or moving the chain end from the middle to the surface of the core) the effective length of chain is halved.

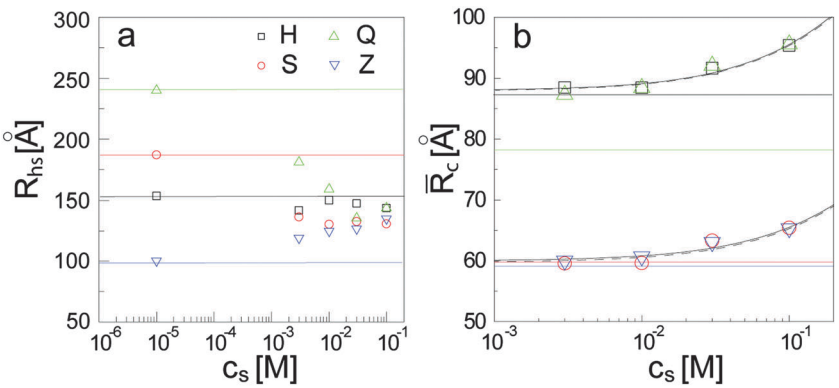

Fig. 3 (a) The effective hard sphere radius and (b) the average core size as a function of the salt concentration. Molecular architectures are denoted by symbols. Horizontal lines indicate the values for no salt conditions. Solid and dashed lines refer to the prediction using either ν = 0.57 or ν = 1/3. All symbols are the same for a and b, σ = 11 Å (S and Z samples) and 15 Å (H and Q samples).

To keep the energy constant, the radius of the PI core will be transformed accordingly to $R_c \mapsto 2^{-1/2} R_c$. Therefore, we come to the factor $\sqrt{2} \simeq 1.41$ that is comparable to the experimental ratio of core sizes of micelles formed with and without PI end-capped macrosurfactants (Fig. 3b).

For a given length of corona chains, $N_{PS}/N_{PI} < 1$, the increase of the core size with the addition of salts as in our case be well explained by the core–solvent surface tension increment driven by the dielectric discontinuity between the core and the solvent.[24,25] It is also possible that the solvent quality affected by ions' solvation may also lead to the increase of the core size. Although these two mechanisms can be distinguished in the limits of crew-cut ($N_{PS}/N_{PI} \ll 1$) or star-like ($N_{PS}/N_{PI} \gg 1$) micelles when the effect of corona is negligible[26,27] or the surface energy is small respectively[27,28] in our case the salt effects on the interfacial tension can alone well explain the data.

Following references 26, 27 and 29, the scaling model for polymer brushes predicts the so-called planar regime. The sizes of the core and the corona scale as $R_c \sim 3^{1/(1+2\nu)} N_{PI} (\gamma/N_{PS})^{2\nu/(1+2\nu)}$ and $R_s \sim (N_{PS}/\gamma)^{3\nu/(1+2\nu)}$ respectively. The interfacial tension at low salt concentrations between the micelle core and the electrolytic solvent is provided by the canonical route for surface tension,[30]

$$\gamma = \gamma_0 + \frac{l_B R T 10^6 c_s}{2} I\left(l_B \kappa^{-1}/2\right), \tag{2}$$

measured in mN m^{-1} and given for planar geometry with

$$I(x) = 2K_0\left(2\sqrt{x}\right){}_1F_2(1; 2/3, 5/3; x) + 3\sqrt{x}K_1\left(2\sqrt{x}\right){}_1F_2(1; 5/3, 5/3; x). \tag{3}$$

Here, K_ν is the modified Bessel function of order ν, and ${}_1F_2$ is the generalized hypergeometric function. $l_B = q^2/4\pi\varepsilon_0\varepsilon k_B T$ is the Bjerrum length and $\kappa^{-1} = (8\pi N_A l_B 10^3 c_s)^{-1/2}$ the Debye screening length of ions in the solvent. $R = k_B N_A$ is the gas constant, and $x = l_B\kappa^{-1}/2$. c_s is measured in moles per liter, ε_0 is the permittivity of free space, and $N_A = 6.022 \times 10^{23}$ is the Avogadro number. The effect of salts, and therefore the second term in eqn (2), becomes significant at small interfacial tension γ_0. For very low salt concentrations, the increase in the surface tension reduces to the Onsager–Samaras limiting law.[31] For considering the ion size and its hydrophobicity, partitioning of ions between the two phases, more elaborated models have been developed.[24,32–34]

Fitting $\bar{R}_c$ with $l_B = 1.4$ nm as for DMAc at room temperature and $\kappa^{-1} = 0.212/\sqrt{c_s(\mathrm{M})}$ nm to the experimental data, Fig. 3b, unveils $\gamma_0 = 1.14$ mN m^{-1} and $\nu = 0.57$ for all the micellar solutions. For a poor solvent, $\nu = 1/3$, the fitting reveals a slightly smaller value of the surface tension, $\gamma_0 = 0.84$ mN m^{-1}. Both values for the core radius exponent ν (0.57 or 1/3) provide good agreement with the experimental data (solid and dashed lines in Fig. 3b) that it thus insensitive to variations in core–solvent quality.

Normally, for dried micellar cores one would proceed as directly fitting data with eqn (1) using the appropriate scattering densities for all (deuterated or non-deuterated) polymer blocks and solvents of a given sample. This is, however, not enough here. In the present case, we should have some solvents in the core since we are in the limit of weak aggregation. Usually, to circumvent this problem, a polymer–solvent concentration profile is arbitrarily imposed on the micellar core and its width is considered a free fitting parameter. Here, we decided to proceed in a slightly different way and allow the solvent to penetrate all over the core to a certain extent. The amount of solvent homogeneously present in the core is then reflected by the fact that the core contrast is taken as a free fitting parameter. This implies that the radius of the core and scattering contrast of the core can vary independently to mimic the solvent penetration in the core. Sets of spectra were fitted together to ensure coherence of polymer density in the core. Typical amounts of solvents in the core are in the range of 26–56%, and Table 1 lists the values of the core size, aggregation number and the mean solvent fraction in the core. The calculations follow the limit of small q values, where for the corona matching conditions the intensity is given by

$$I_m(q \to 0) = (\rho_{PI} - \rho_{d\text{-}PS})^2 N_{ag} \upsilon_{PI} \phi N_A, \tag{4}$$

where ρ_{PI} is the scattering length density of PI and $\rho_{d\text{-}PS}$ is the scattering length density of d-PS. $\upsilon_{PI} = (0.12 \times 176)$ nm^3 is the volume of the PI block, $\phi = 0.01$. Experimentally, the measured intensity in the limit of small angles provides the value of the aggregation number N_{ag}. The combination of these values with the core radius, $\bar{R}_c$, obtained from the model fit, allows us to obtain the solvent fraction in the core, $f = 1 - 3N_{ag}\upsilon_{PI}/(4\pi\bar{R}_c{}^3)$.[15]

To distinguish between the salt effect on the surface tension and its effect on the solvent quality, the size of corona blocks R_s and the radius of core are extracted from scattering data under no matching conditions for micelles of two different block lengths (PS_{113}-b-PI_{199} and PS_{141}-b-PI_{176}). Experimental data for sample A are displayed in Fig. 2b and c for salt concentrations of 0 M and 0.1 M, respectively. Inspection of those figures clearly demonstrates high quality of model fittings. Parameters extracted from these fittings are used below to construct Fig. 4.

Table 1 Fit results for micelles with corona matching conditions, sample C

Sample	c_s (M)	$I_m(q \to 0)$ (cm^{-1})	R_{hs} (Å)	$\bar{R}_c$ (Å)	N_{ag}	f
CH	0.0	51.0	153.3	87.7	64	0.52
	0.003	51.7	141.8	88.5	65	0.52
	0.01	53.3	149.8	88.4	67	0.51
	0.03	65.5	147.5	91.6	82	0.46
	0.1	60.0	146.5	95.3	76	0.56
CQ	0.0	48.7	240.1	79.1	61	0.37
	0.003	58.2	181.0	87.3	73	0.44
	0.01	65.5	169.5	88.4	82	0.40
	0.03	74.9	155.3	92.0	94	0.39
	0.1	61.8	143.5	95.6	78	0.55
CS	0.0	20.8	187.0	61.1	26	0.42
	0.003	23.3	136.3	59.5	29	0.30
	0.01	22.7	130.3	59.6	29	0.32
	0.03	29.6	132.3	63.3	37	0.26
	0.1	25.2	130.6	65.4	32	0.43
CZ	0.0	20.8	107.4	58.9	26	0.35
	0.003	20.8	119.2	60.0	26	0.38
	0.01	24.8	124.8	60.7	31	0.48
	0.03	27.1	126.8	63.1	34	0.31
	0.1	26.2	134.9	65.3	33	0.40

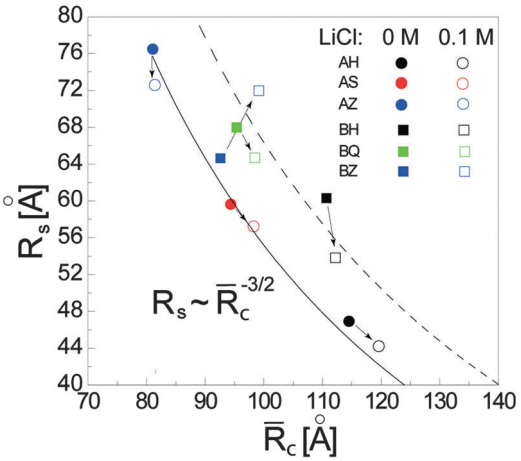

Fig. 4 Size of corona *versus* the core size for micelles with different architectures and block lengths (PS_{113}-*b*-PI_{199}, circles; PS_{141}-*b*-PI_{176}, boxes). Closed and open symbols are the experimental data for solutions without and with the LiCl salt respectively. Lines show scaling $R_s \sim (\bar{R}_c/N_{PI})^{-3/2}$, with κ^{-1} = 6.8 Å.

Fig. 4 collects the values of R_s for PS corona chains against the core radius of micelles, $\bar{R}_c$, noticing that $Li^+$and Cl^- ions increase the size of a core and decrease R_s of a corona simultaneously. Rearranging the scaling laws for R_s and $\bar{R}_c$ provides a relation between these two quantities $R_s \sim \psi(\nu)(\bar{R}_c/N_{PI})^{-3/2}$, whereas $R_s \simeq 2R_g$ and only the pre-factor $\psi(\nu)$ depends on the Flory swelling exponent. This power law is shown in Fig. 4 for micelles formed by PS_{113}-*b*-PI_{199} (solid line) and PS_{141}-*b*-PI_{176} (dashed line). The dashed line is shifted up by a factor of $(199/176)^{3/2} \simeq 1.2$ due to different sizes of PI blocks. Upon addition of salts, new equilibrium values of $\bar{R}_c$ and R_s are established as shown by open symbols. Fig. 4 displays the data of six different micelles, and that as displayed in the $R_s \times \bar{R}_c$ diagram obeys the $\psi(\nu)$ = const line. This implies no change in solvent quality and changes in the micelle dimensions can only be attributed to the surface tension.

Exception is found for BZ sample that, presumably, exhibits a loop in the corona chains as depicted in Fig. 1 before addition of salts. Upon addition of salts, the loop is probably released and the sample BZ displaces outwards the $\psi(\nu)$ = const curve in the $R_s \times \bar{R}_c$ diagram (shown by the arrow) as its corona extends.

In this work we investigated the self-assembly of non-ionic and ionic macro-surfactants in a weak selective polar solvent. We have shown unambiguously that for the systems studied here, the addition of salts to the solution changes significantly the core–solvent interfacial energy by a mechanism that is highly governed by the induction of virtual charges at the interface. The approach developed here that combines the scaling theory of micelle formation and results of canonical calculations for salt effects on the surface tension successfully explains the variation of the micelle structure for several copolymer architectures and solution conditions. We expect our approach to be applicable for a wide range of systems self-assembled in weakly selective solvents.

References

1 A. Blanazs, S. P. Armes and A. J. Ryan, *Macromol. Rapid Commun.*, 2009, **30**, 267.
2 M. Ballauff and O. Borisov, *Curr. Opin. Colloid Interface Sci.*, 2006, **11**, 316.
3 M. Ballauff, *Prog. Polym. Sci.*, 2007, **32**, 1135.
4 S. Förster and M. Antonietti, *Adv. Mater.*, 1998, **10**, 195.
5 R. R. Netz, *Europhys. Lett.*, 1999, **47**, 391.
6 E. B. Zhulina and O. V. Borisov, *Macromolecules*, 2012, **45**, 4429.
7 O. V. Borisov, E. B. Zhulina, F. A. M. Leermakers, M. Ballauff and A. H. E. Müller, *Adv. Polym. Sci.*, 2011, **241**, 1.
8 H. Shen and A. Eisenberg, *J. Phys. Chem. B*, 1999, **103**, 9473.
9 L. F. Zhang, K. Yu and A. Eisenberg, *Science*, 1996, **272**, 1777.
10 Y. Mai and A. Eisenberg, *Chem. Soc. Rev.*, 2012, **41**, 5969.
11 G. V. Jensen, Q. Shi, G. R. Deen, K. Almdal and J. S. Pedersen, *Macromolecules*, 2012, **45**, 430.
12 F. Muller, G. Romet-Lemonne, M. Delsanti, J. W. Mays, J. Daillant and P. Guenoun, *J. Phys.: Condens. Matter*, 2005, **17**, S3355.
13 K. Binder, M. Muller, F. Schmid and A. Werner, *Macromol. Symp.*, 1999, **139**, 1.
14 Y. Liu, S.-H. Chen and J. S. Huang, *Macromolecules*, 1998, **31**, 2236.
15 R. Lund, L. Willner, P. Lindner and D. Richter, *Macromolecules*, 2009, **42**, 2686.
16 V. Schädler, J. Spickermann, H. J. Räder and U. Wiesner, *Macromolecules*, 1996, **29**, 4865.
17 K. Nasirzadeh, R. Neueder and W. Kunz, *J. Chem. Thermodyn.*, 2005, **37**, 331.
18 E. Di Cola, C. Lefebvre, A. Deffieux, T. Narayanan and R. Borsali, *Soft Matter*, 2009, **5**, 1081.
19 E. Mendes, V. Schädler, C. M. Marques, P. Lindner and U. Wiesner, *Europhys. Lett.*, 1997, **40**, 521.
20 J. S. Pedersen, C. Svaneborg, K. Almdal, I. W. Hamley and R. N. Young, *Macromolecules*, 2003, **36**, 416.
21 J. S. Pedersen and M. C. Gerstenberg, *Macromolecules*, 1996, **29**, 1363.
22 J. K. Percus and G. J. Yevick, *Phys. Rev.*, 1958, **110**, 1.
23 A. V. Korobko, W. Jesse, S. U. Egelhaaf, A. Lapp and J. R. C. van der Maarel, *Phys. Rev. Lett.*, 2004, **93**, 177801.
24 Y. Levin and J. E. Flores-Mena, *Europhys. Lett.*, 2001, **56**, 187.
25 R. A. Curtis and L. Lue, *J. Chem. Phys.*, 2005, **123**, 174702.
26 A. Halperin, *Macromolecules*, 1987, **20**, 2943.
27 C. M. Marques, J.-F. Joanny and L. Lebler, *Macromolecules*, 1988, **21**, 1051.
28 S. Huissmann, R. Blaak and C. N. Likos, *Macromolecules*, 2009, **42**, 2806.
29 T. M. Birshtein and E. B. Zhulina, *Polymer*, 1989, **30**, 170.
30 Y. Levin, *J. Chem. Phys.*, 2000, **113**, 9722.
31 L. Onsager and N. N. T. Samaras, *J. Chem. Phys.*, 1934, **2**, 528.
32 Y. Levin, A. P. dos Santos and A. Diehl, *Phys. Rev. Lett.*, 2009, **103**, 257802.
33 M. Bier, J. Zwanikken and R. van Roij, *Phys. Rev. Lett.*, 2008, **101**, 046104.
34 A. Onuki, *J. Chem. Phys.*, 2008, **128**, 224704.